sEffects of DEM Sources on Hydrological Modeling: Case Study of Upstream Area in Bang Pakong River Basin,Thailand

Pyay Thar[1], Pongsit Polsomboon[1], Teerawat Ram-Indra[1] and Piyatida Ruangrassamee[1*]

[1] *Department of Water Resources Engineering, Faculty of Engineering, Chulalongkorn University, Bangkok, THAILAND*
**Corresponding author; E-mail address: Piyatida.H@chula.ac.th*

Abstract

Digital Elevation Models (DEMs) are essential tools in hydrological and geomorphological studies, providing topographic data for watershed analysis, streamflow simulation, and flood modeling. This study evaluates the performance of two global DEMs— Hydrological data and maps based on SHuttle Elevation Derivatives at multiple Scales (HydroSHEDS) and Multi-Error-Removed Improved-Terrain Hydro (MERIT Hydro) with spatial resolution of 500m by utilizing the Rainfall-Runoff-Inundation (RRI) model to simulate daily discharge in the upstream area of Bang Pakong River basin, Thailand The differences in elevation and flow accumulation were investigated. Model calibration was performed using data from 2021, and validation was conducted with data from 2019, assessing the accuracy of each DEM source in capturing streamflow dynamics. Statistical metrics, including the Nash-Sutcliffe Efficiency (NSE), coefficient of determination (R^2), and Root Mean Square Error (RMSE), are employed to evaluate model performance. Results indicate that both DEMs effectively capture the overall hydrograph pattern, but their effectiveness varies across different stations. The prominent difference in the elevation especially in mountainous areas. The difference in flow accumulation demonstrates different river channel position derived from each DEM. The findings provide insights into the selection of appropriate DEMs for hydrological modeling in the region, contributing to improved water resources management and flood prediction capabilities.

Keywords**:** HydroSHEDS; MERIT-Hydro; Flow Accumulation; Rainfall Runoff Inundation Model; Bang Pakong River Basin.

1. Introduction

A digital elevation model (DEM) serves as a grid-based depiction of the Earth's terrain and is utilized across various fields of research and land management[1]. Digital Elevation Model (DEM) is a crucial factor to evaluate in any procedure that employs topographic analysis, along with its associated characteristics such as slope, curvature, roughness, drainage area, and network. It has been utilized in various scientific fields, including hydrology, geology, geomorphology, development, urban planning, and surveying[2-4]. The hydrogeomorphic characteristics of a watershed, including flow directions, stream networks, and catchment boundaries, are crucial inputs for various hydrological applications and are often obtained from these models [1, 5, 6].

Numerous initiatives have aimed to substitute conventional topographic models, which depend on field surveys, with remote-sensing methods like satellite imaging for gathering elevation data to create Digital Elevation Models (DEMs). The integration of remote-sensing techniques and sophisticated computational approaches has transformed the process of obtaining and accessing DEM datasets from spaceborne or airborne Light Detection and Ranging (LiDAR), significantly enhancing the available data resources [7-9]. Additionally, the travel time of surface flow, groundwater movement, and runoff properties are significantly influenced by the geomorphological features of the terrain [10]. Consequently, effective and dependable hydrological modeling requires a thorough understanding of the surface topography [11].

The automated calculation of hydrological and morphometric parameters for any watershed is influenced not only by the resolution of the Digital Elevation Model (DEM) but also by the sources from which the data is derived [12].

Numerous hydrological and hydraulic models, including SWAT (Soil and Water Assessment Tool), MIKE SHE (System Hydrologique European), HEC-RAS (Hydrologic Engineering Center's-River Analysis System) and RRI (Rainfall-Runoff Inundation Model), have been developed to assess different geomorphological and hydrological parameters within a watershed [13-15]. Many of these models utilize Digital Elevation Models (DEMs) as their main input, which can be accessed for free from various online platforms offering different spatial resolutions. Consequently, selecting an appropriate DEM from the numerous available sources has become a challenging task [12].

DEMs have progressed significantly, integrating advanced technologies and methodologies to improve both accuracy and coverage. This study analyzes two widely utilized and freely accessible global DEMs. Which are HydroSHEDS and MERIT-Hydro. HydroSHEDS was developed in 2009 using elevation data from the Shuttle Radar Topography Mission (SRTM), which operates at a resolution of 3 arc-seconds. The primary process involved hydrological conditioning, which includes techniques for void-filling, filtering, stream burning, and upscaling [16]. MERIT Hydro, launched in 2019, is a hydrologically refined Digital Elevation Model (DEM) that was created by eliminating several error components from the SRTM3 [17] and Advanced Land Observing Satellite ALOS World 3D – 30m (AW3D30) DEMs [18]. This model integrates various surface water datasets and corrections to enhance the accuracy of hydrological information [19]. This study aims to evaluate the effects of these two different DEM sources on stream flow simulation using Rainfall Runoff Inundation (RRI) model.

2. Study Area

The Bang Pakong River basin is one of Thailand's key river systems, situated in the eastern part of the country between latitudes 13°05'-14°30'N and longitudes 100°57'-102°00'E, covering an area of around (7417) km² and connected to the Gulf of Thailand Fig 1. The River Basin is comprised of four sub-basins: the Main Bang Pakong River, Nakhon Nayok River, Khlong Tha Lat, and part of Khlong Luang while the Prachinburi River Basin is made up of four sub-basins: Khlong Phra Sathung, Khlong Phra Prong, Mae Nam Hanuman, and the Main Prachinburi sub-basin **[20]**. The main river stretches about 240 km in length and is divided into the upper Prachinburi River basin and the lower Bang Pakong River basin. The upper Prachinburi River flows through hilly terrain, while the lower areas feature flat, low-lying alluvial plains, ideal for rice cultivation and other agricultural activities. This study will focus the upper catchment which provides abundant water during the wet season [21].

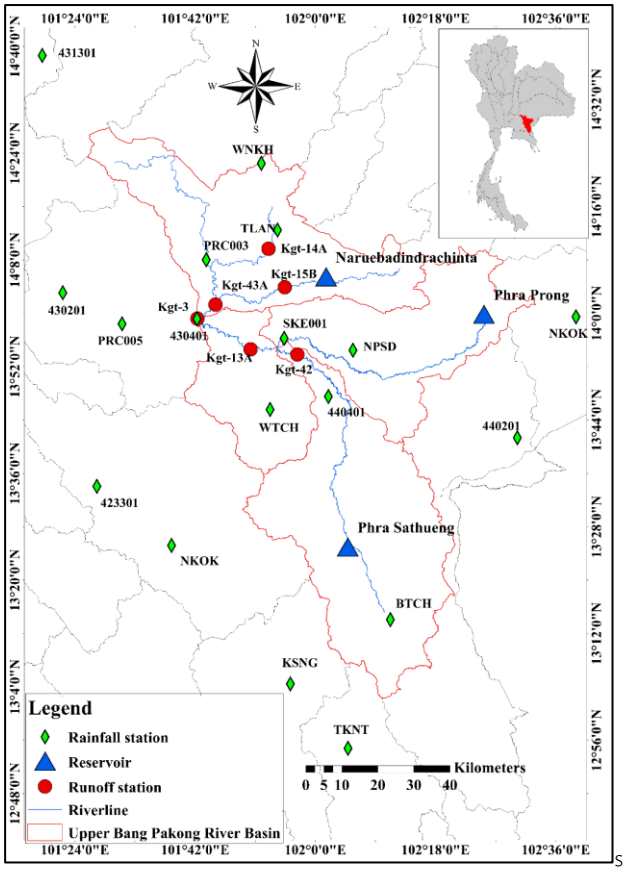

Fig. 1 Location of the Upstream area of Bang Pakong River Basin.

The Bang Pakong basin has a tropical monsoon climate, characterized by a north-easterly monsoon during the dry season from November to April, and a south-westerly monsoon during the wet season from May to October [22]. Rainfall in the Bang Pakong basin generally ranges between 1,000 and 2,000 mm, with the majority of runoff (8.6 billion cubic meters or Bm³) produced in the northern subbasins, including Nakhon Nayok, main Prachin Buri, and Hanuman, accounting for 60% of the total. Only 10% of the runoff occurs during the dry season [23]. During the wet season, flood-prone areas in the Bang Pakong basin are primarily located in the lower part of the Nakhon Nayok River sub-basin [20].

3. Data and Methodology

3.1 Data Description

In this study, various datasets were required for processing

and calibrating the RRI model. The dataset used was downloaded from and provided by related sources, as shown in Table 1. The study utilized daily rainfall data from 6 stations of Thai Meteorological Department (TMD) and 12 stations of Hydro-Informatics Institute (HII) in the flood event years of 2019 and 2021. To simulate the RRI model, six observed runoff stations from the Royal Irrigation Department (RID) which are Kgt-3, Kgt-13A, Kgt-14A, Kgt-15B, Kgt-42 and Kgt-43A were selected for comparison with the simulated results. The flows originating from three upstream reservoirs which are Khlong Phra Sathueng, Pra Pong and Naruebodindrachinta reservoirs were considered in the RRI model simulation. The DEMs of 500 m resolutions from HydroSHEDS and MERIT-Hydro utilized in this study are shown in Fig 2. The land use data for this study showed in Fig 3. has five main land covers (Agriculture, Forest, Shrubland, Urban and Water) and was obtained from the Land Development Department (LDD) of Thailand.

Table 1 List of all datasets and sources used in this study

Data	Resolution/ Scale	Year	Source
Observed rainfall	Daily	2019 & 2021	TMD, HII
Digital Elevation Modal (DEM)	500m	2009	Hydro SHEDS
	500m	2014	MERIT-Hydro
Land use	-	2018	LDD
Observed streamflow	Daily	2019 & 2021	RID
Surveyed river cross section		-	RID
Observed release	Daily	2019 & 2021	RID

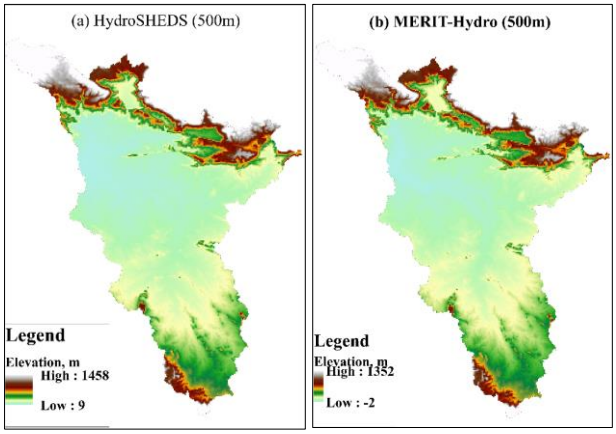

Fig. 2 DEM maps of the Upstream area of Bang Pakong River Basin

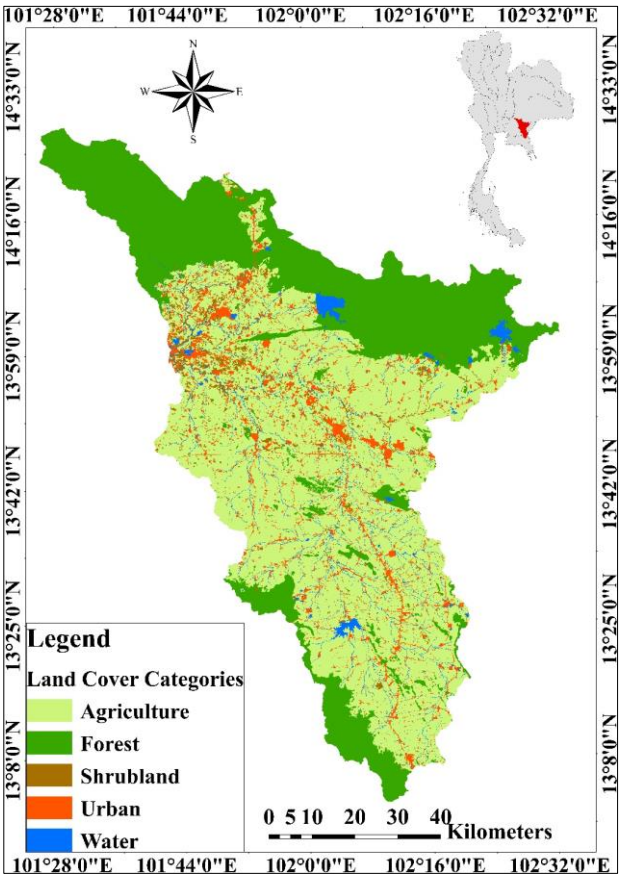

Fig. 3 Land Use Map of Upstream area of Bang Pakong River Basin (Source: LDD)

3.2 Methodology

3.2.1 Rainfall-Runoff-Inundation Model

The flood simulation in this study employed a two-dimensional Rainfall-Runoff-Inundation (RRI) model shown in Fig 4 which deals separately with surface flow, named slope, and river channels. [24].

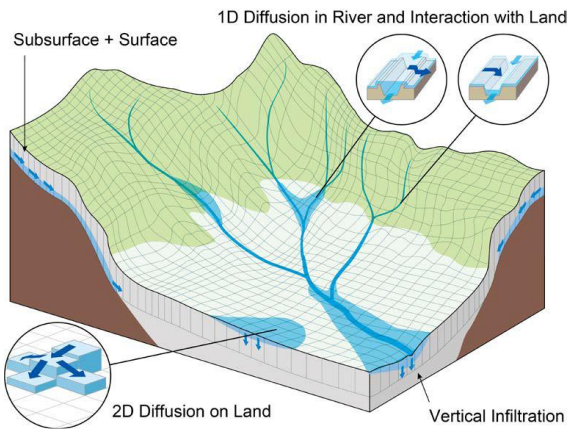

Fig. 4 Schematic diagram of Rainfall-Runoff-Inundation (RRI) Model [24]

The river channel is situated within a grid cell, and the model presumes that both the slope and the river are contained within this same grid cell. The channel is represented as a single vector that runs along the centerline of the slope grid cell above it. This channel serves as an additional flow pathway connecting the grid cells that follow the actual course of the river, as illustrated in Fig. 4. Lateral flows are simulated for slope cells on a two-dimensional basis. The governing equations of slope computation are derived based on the following mass balance Eq. (1) and momentum Eqs. (2) and (3) for gradually varied unsteady flow:

$$\frac{\partial \mathrm{h}}{\partial \mathrm{t}} + \frac{\partial \mathrm{qx}}{\partial \mathrm{x}} + \frac{\partial \mathrm{qy}}{\partial \mathrm{y}} = r - f \quad (1)$$

$$\frac{\partial qx}{\partial \mathrm{t}} + \frac{\partial \mathrm{uqx}}{\partial \mathrm{x}} + \frac{\partial \mathrm{vqy}}{\partial \mathrm{y}} = -gh\frac{\partial \mathrm{H}}{\partial \mathrm{x}} - \frac{\tau x}{\rho w} \quad (2)$$

$$\frac{\partial qy}{\partial t} + \frac{\partial uqx}{\partial x} + \frac{\partial vqy}{\partial y} = -gh\frac{\partial H}{\partial y} - \frac{\tau x}{\rho w} \quad (3)$$

where h is the height of water from the local surface, qx and qy are unit width discharge in the x and y directions, u and v are flow velocities in the x and y directions, r is rainfall intensity, H is the height of water from a datum, ρw is the density of water, g is gravitational acceleration, and τx and τy are shear stress in the x and y directions. Second terms on the right side of Eqs. (2) and (3) are calculated using Manning's equation. To solve the two-dimensional equation, the RRI model adopts diffusive wave approximation.

The RRI model calculates stream flow at river grid cells with one-dimensional diffusive wave. The river geometry is assumed to be rectangle, whose shapes are noted by width W (m) and depth D (m) as the following equations:

$$W = CWA^{SW} \quad (5)$$

$$D = CDA^{SD} \quad (6)$$

where *D* is the depth [m], *W* is the width [m], *A* is the area [km2], *Cd* and *Sd* are the depth parameters, and *Cw* and *Sw* are the width parameters.

The vertical infiltration term is more important for mountainous areas and is related to the relationship between the discharge and hydraulic gradient, which is sensitive to generating both surface and subsurface flows. Vertical infiltration can be treated as infiltration loss with the Green–Ampt infiltration model [25].

$$f = kv\left[1 + \frac{(\phi - \theta i)Sf}{F}\right] \quad (7)$$

where *f* is infiltration loss [mm/h], *kv* is the vertical hydraulic conductivity [m/s], ϕ is soil porosity, θ *i* is the initial water volume content, *F* is the cumulative infiltration depth [m], and *Sf* is the wetting front suction head [m].

3.2.2 RRI Model Setup

The input datasets for the RRI model consist of five categories: rainfall data, topographical information (including digital elevation model, flow direction, and flow accumulation), land use, river geometry and reservoir outflow. After setting up the model with the required data, the flood event years of 2021 and 2019 are selected for calibration and validation resulting in the output of river discharge to evaluate the performance of HydroSHEDS and MERIT-Hydro DEMs. Model parameters were adjusted and sensitive parameters were identified. The comprehensive procedures for the setup and execution of RRI modeling are illustrated in Fig 5.

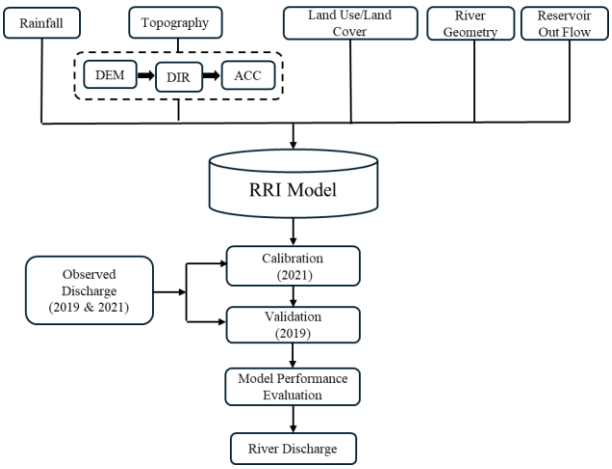

Fig. 5 Flow chart of RRI model set up

4. Results and Discussion

4.1 Comparative Analysis of DEM and Flow Accumulation between HydroSHEDS and MERIT-Hydro DEMs

Most of the areas show good agreement within ±10 m between the two DEMs as shown in Fig 6. Significant discrepancies are found mostly in mountainous and hilly regions and along river channels where HydroSHEDS has higher elevation than MERIT-Hydro. For the flow accumulation, the primary distinctions between the two DEMs are predominantly located

along the main river channels as shown in Fig 7. The difference of the flow accumulation demonstrates the different river channel position derived from each DEM. The light dark green colour indicates the river channel position derived from HydroSHEDS and the yellow and red colours indicate the river channel position derived from MERIT-Hydro.

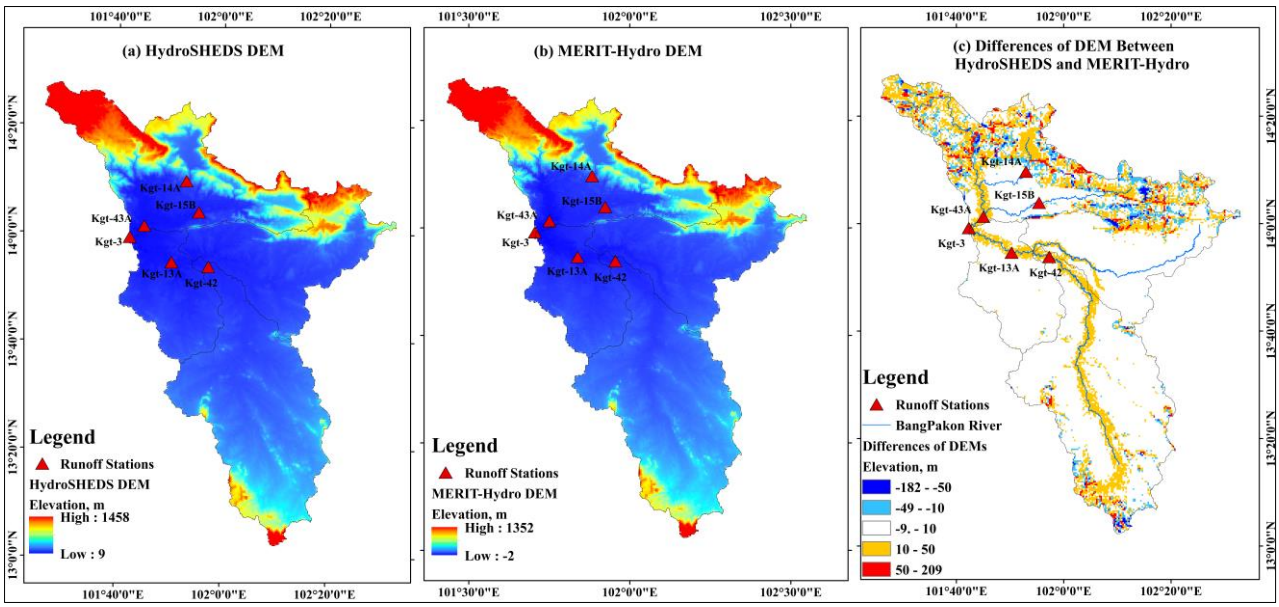

Figure. 6 Comparison of DEM between HydroSHEDS and MERIT-Hydro DEMs

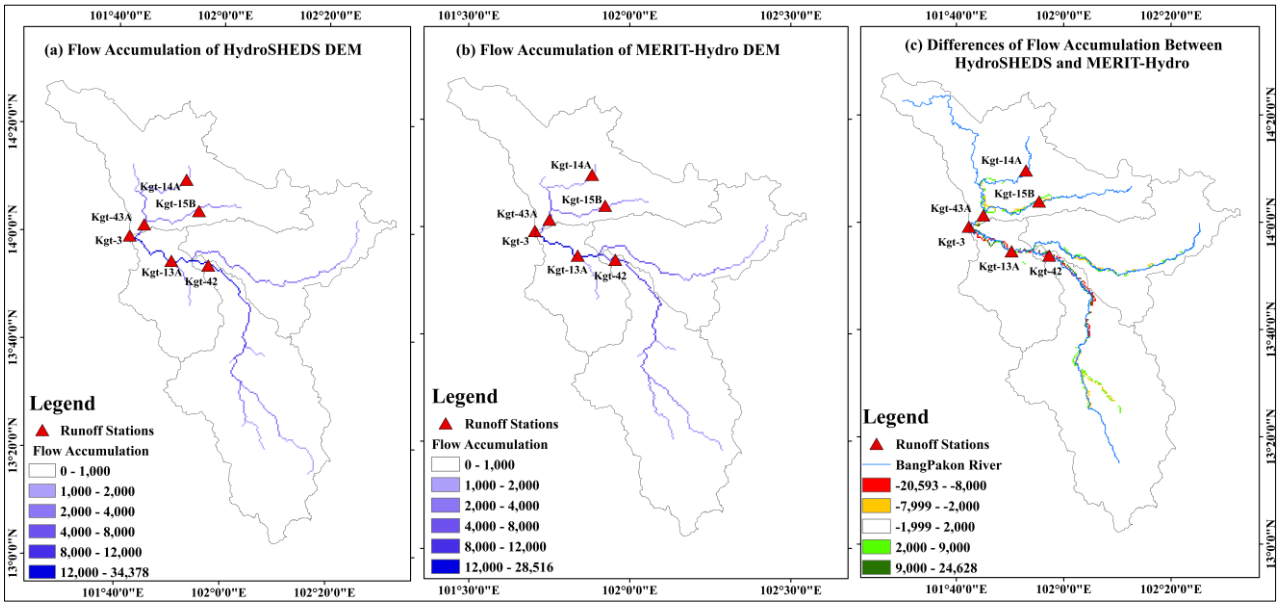

Figure. 7 Comparison of Flow Accumulation between HydroSHEDS and MERIT-Hydro DEM

4.2 Effect of River Thresholds

In this study, the effect of river threshold was also investigated. Three river thresholds of 20, 50, and 100 were analyzed. It was found that the effect of the river threshold is on peak flow as shown in Fig 8. The example of the simulated discharge of station Kgt-43A using regression equations for river cross section demonstrates that the higher the river threshold, the lower the peak flow since the higher river threshold captures more tributary network. The most prominent differences occur at the peaks around late August to early September.

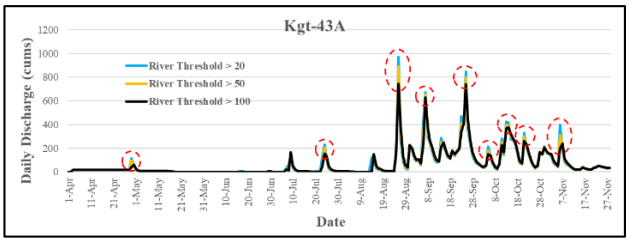

Fig. 8 Comparison of Different River Thresholds at Kgt-43 station in 2021

4.3 Model Calibration

The results of model calibration for 2021 are presented in Fig 8. In the calibration process, it is found that the sensitive parameters are the hydraulic conductivity, the Manning's roughness coefficient (n) and the soil depth. The calibrated hydraulic conductivity (ksv) ranges from 2.78×10^{-7} to 1.67×10^{-6} according to the five land use types, the Manning's roughness coefficient (n) is 0.04 and the soil depth is 2.2 m. According to the hydrograph results, the simulation discharge at each station for both DEMs shows good correlation with the observed data in the dry season except for station Kgt-42 for MERIT-Hydro DEM. Although the general shape of the hydrograph at each station is captured well by the model, it struggles to simulate the timing and magnitude of the multiple peaks and fluctuations of the 2021 events. The simulated results at station Kgt-3, Kgt-13A and Kgt-15B are overestimated than the observed discharge at the peak discharge during the rainy season for both DEMs while that of station Kgt-14A and Kgt-43A are underestimated. Although station Kgt-42 has good correlation with the observed discharge in the rainy season, it also shows the temporal fluctuations for both DEMs.

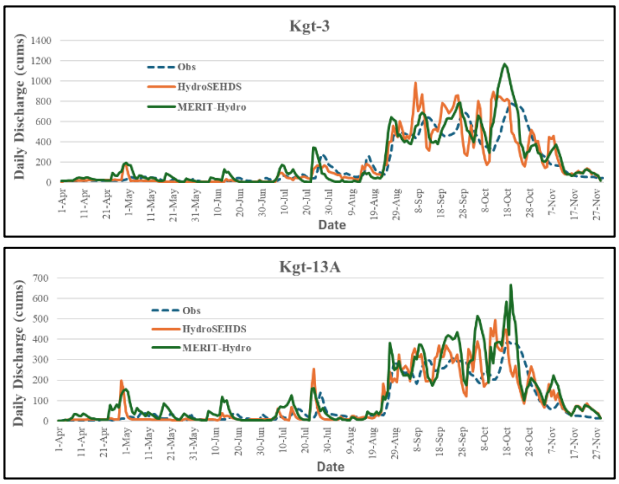

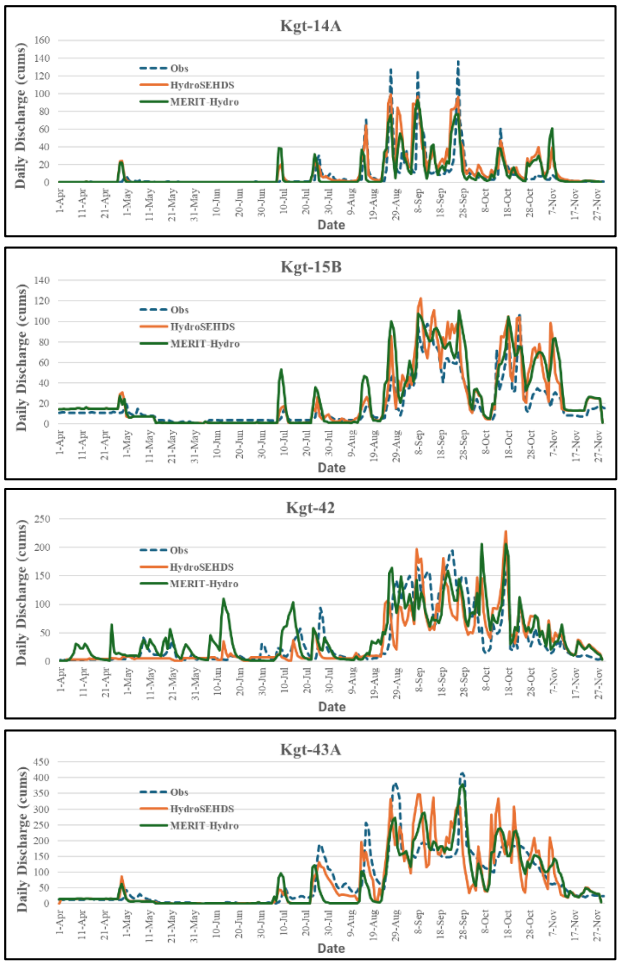

Fig. 9 Comparison of observed and simulated discharges using HydroSHEDS and MERIT-Hydro DEMs for the calibration process in 2021.

Based on the statistical performance shown in Table 2, MERIT-Hydro outperforms HydroSHEDS at some stations (Kgt-3 and Kgt-43A), while HydroSHEDS performs better at others (Kgt-13A, Kgt-15B, Kgt-42). At Kgt-14A the models show similar performance.

Table 2 Summary of model performance from the calibration process in 2021. Variables: NSE(Nash-Sutcliffe Efficiency Index), R^2 (Coefficient of Determination) and RMSE(Root Mean Square Error)

Station	HydroSHEDS			MERIT-Hydro		
	NSE	R^2	RMSE (m^3/s)	NSE	R^2	RMSE (m^3/s)
Kgt-3	0.57	0.67	147.68	0.65	0.75	132.49
Kgt-13A	0.63	0.70	68.19	0.53	0.76	76.53
Kgt-14A	0.41	0.57	14.45	0.40	0.48	14.46
Kgt-15B	0.53	0.79	15.33	0.42	0.77	16.98
Kgt-42	0.55	0.58	32.51	0.53	0.58	33.23
Kgt-43A	0.51	0.59	59.95	0.66	0.70	49.96

4.4 Model Validation

The streamflow simulations using HydroSHEDS and MERIT-Hydro DEMs show a general ability to capture the seasonal patterns of discharge across the with both models demonstrating varying degrees of success in matching observed peak flows and baseflow levels; HydroSHEDS tends to overestimate peak discharge at Kgt-3 and Kgt-13A, while both models underestimate peak flows at Kgt-14A, whereas for Kgt-15B, Kgt-42, and Kgt-43A, the models performed relatively well with slight overestimations and underestimations shown in Fig 9.

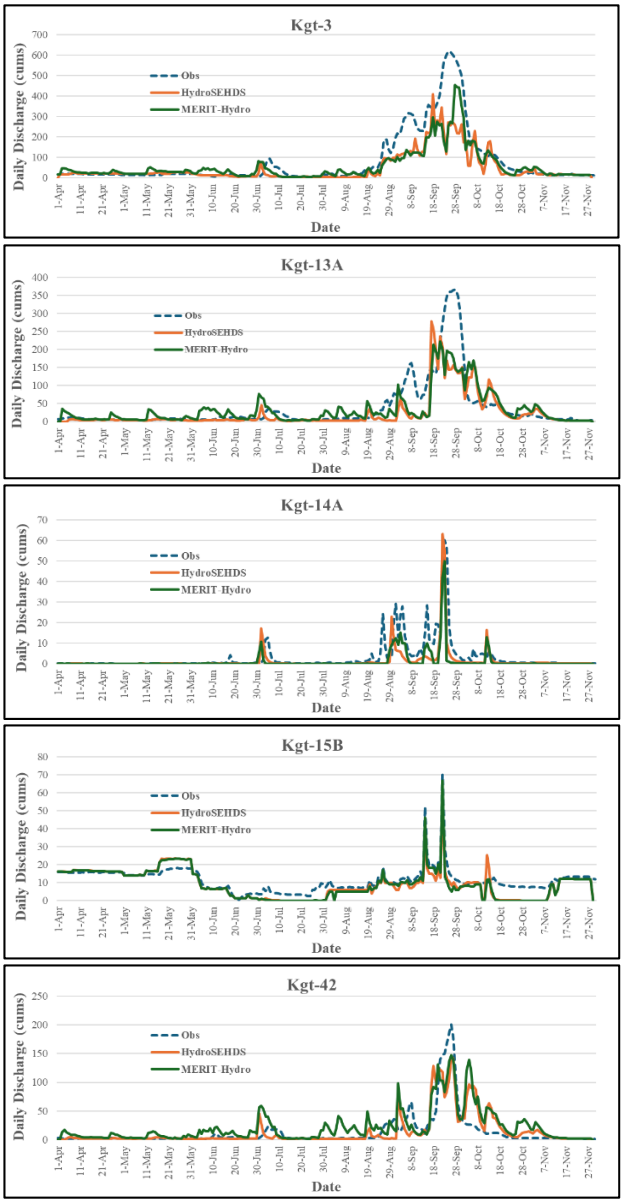

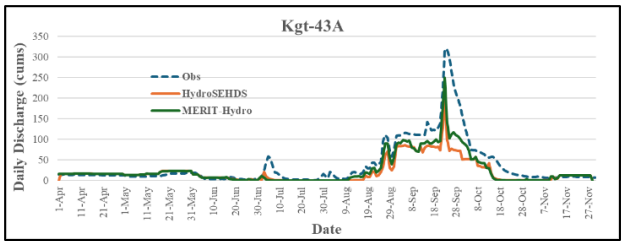

Fig. 9 Comparison of Observed and simulated discharge using HydroSHEDS and MERIT-Hydro DEMs for the validation process in 2019

5. Conclusion

The study aims to evaluate the impact of the two widely used DEMs which are HydroSHEDS and MERIT-Hydro on streamflow simulation using the Rainfall-Runoff-Inundation (RRI) model within the Bang Pakong River Basin. HydroSHEDS tends to show higher elevations than MERIT-Hydro, particularly in the mountainous areas. The difference of the flow accumulation demonstrates the difference of the river channel position derived from each DEM. The effect of the river threshold is on the peak flow. The higher the river threshold results in the lower the peak flow since the higher river threshold captures more tributary network. From the calibration, it is found that the sensitive parameters are the hydraulic conductivity, the Manning's roughness coefficient (n) and the soil depth. Based on the simulation results, it reveals that both HydroSHEDS and MERIT-Hydro DEMs exhibit varying performance in simulating streamflow across different stations; HydroSHEDS generally overestimates peak discharge at Kgt-3 and Kgt-13A while both DEMs underestimate peak flow at Kgt-14A yet demonstrate reasonable performance with slight overestimations or underestimations at stations Kgt-15B, Kgt-42, and Kgt-43A. These findings underscore the importance of considering local terrain characteristics and data quality when choosing a DEM for hydrological modeling. Additionally, further research should investigate effect of DEM resolution with different hydrological models and spatial and temporal contribution of flood peaks to identify appropriate mitigation measures.

Acknowledgement

The authors gratefully acknowledge the data provided by Thai Meteorological Department, Royal Irrigation Department, Hydro Informatics Institute, and Land Development Department. The first auhtor is supported by Chulalongkorn University's Graduate Scholarship Programme for ASEAN or Non-ASEAN Countries. The authors would like to acknowledge a partial funding and support from Department of Water Resources Engineering, Faculty of Engineering, Chulalongkorn University. The authors also would like to thank the reviewers for their constructive comment.

References

[1] Freitas, H. R. d. A., Freitas, C. d. C., Rosim, S., & Oliveira, J. R. d. F. (2016). Drainage networks and watersheds delineation derived from TIN-based digital elevation models. *Computers & Geosciences*, *92*, 21-37. https://doi.org/https://doi.org/10.1016/j.cageo.2016.04.003

[2] Fraser, C., B, E., & Gruen, A. (2002). ARTICLE IN PRESS 1 Processing of Ikonos imagery for submetre 3D positioning and 2 building extraction. *ISPRS Journal of Photogrammetry and Remote Sensing*, *56*, 177-194. https://doi.org/10.1016/S0924-2716(02)00045-X

[3] Lee, S.-J., Komatitsch, D., Huang, B.-S., & Tromp, J. (2009). Effects of Topography on Seismic-Wave Propagation: An Example from Northern Taiwan. *Bulletin of the Seismological Society of America*, *99*. https://doi.org/10.1785/0120080020

[4] Pakoksung, K., & Takagi, M. (2015). Digital elevation models on accuracy validation and bias correction in vertical. *Modeling Earth Systems and Environment*, *2*. https://doi.org/10.1007/s40808-015-0069-3

[5] Uuemaa, E., Hughes, A. O., & Tanner, C. C. (2018). Identifying Feasible Locations for Wetland Creation or Restoration in Catchments by Suitability Modelling Using Light Detection and Ranging (LiDAR) Digital Elevation Model (DEM). *Water*, *10*(4), 464. https://www.mdpi.com/2073-4441/10/4/464

[6] Ye, S., Zhang, Q., Yan, F., Ren, B., & Shen, D. (2022). A novel approach for high-quality drainage network extraction in flat terrains by using a priori knowledge of hydrogeomorphic features to extend DEMs: A case study in the Hoh Xil region of the Qinghai-Tibetan Plateau. *Geomorphology*, *403*, 108138. https://doi.org/https://doi.org/10.1016/j.geomorph.2022.108138

[7] Keys, L., & Baade, J. (2019). Uncertainty in Catchment Delineations as a Result of Digital Elevation Model Choice. *Hydrology*, *6*(1), 13. https://www.mdpi.com/2306-5338/6/1/13

[8] Magruder, L., Neuenschwander, A., & Klotz, B. (2021). Digital terrain model elevation corrections using space-based imagery and ICESat-2 laser altimetry. *Remote Sensing of Environment*, *264*, 112621. https://doi.org/https://doi.org/10.1016/j.rse.2021.112621

[9] Kmoch, A., Klug, H., Ritchie, A. B. H., Schmidt, J., & White, P. A. (2016). A Spatial Data Infrastructure Approach for the Characterization of New Zealand's Groundwater Systems. *Transactions in GIS*, *20*(4), 626-641. https://doi.org/https://doi.org/10.1111/tgis.12171

[10] Zhang, J., Condon, L. E., Tran, H., & Maxwell, R. M. (2021). A national topographic dataset for hydrological modeling over the contiguous United States. *Earth Syst. Sci. Data*, *13*(7), 3263-3279. https://doi.org/10.5194/essd-13-3263-2021

[11] Moges, D. M., Virro, H., Kmoch, A., Cibin, R., Rohith, A. N., Martínez-Salvador, A., Conesa-García, C., & Uuemaa, E. (2023). How does the choice of DEMs affect catchment hydrological modeling? *Science of The Total Environment*, *892*, 164627. https://doi.org/https://doi.org/10.1016/j.scitotenv.2023.164627

[12] Munoth, P., & Goyal, R. (2019). Effects of DEM Source, Spatial Resolution and Drainage Area Threshold Values on Hydrological Modeling. *Water Resources Management*, *33*(9), 3303-3319. https://doi.org/10.1007/s11269-019-02303-x

[13] Jayakumar, D., & Kumar, D. (2016). Comparison of digitally delineated stream networks from different spaceborne digital elevation models: A case study based on two watersheds in South India. *Arabian Journal of Geosciences*, *9*, 710. https://doi.org/10.1007/s12517-016-2726-x

[14] Pakoksung, K., & Takagi, M. (2021). Assessment and comparison of Digital Elevation Model (DEM) products in varying topographic, land cover regions and its attribute: a case study in Shikoku Island Japan. *Modeling Earth Systems and Environment*, *7*(1), 465-484. https://doi.org/10.1007/s40808-020-00891-x

[15] Reddy, A., & Janga Reddy, M. (2015). Evaluating the influence of spatial resolutions of DEM on watershed runoff and sediment yield using SWAT. *Journal of Earth System Science*, *124*, 1517-1529. https://doi.org/10.1007/s12040-015-0617-2

[16] Lehner, B., Verdin, K., & Jarvis, A. (2006). HydroSHEDS technical documentation. *World Wildlife Fund US, Washington, DC*, *5*.

[17] Farr, T. G., Rosen, P. A., Caro, E., Crippen, R., Duren, R., Hensley, S., Kobrick, M., Paller, M., Rodriguez, E., Roth, L., Seal, D., Shaffer, S., Shimada, J., Umland, J., Werner, M., Oskin, M., Burbank, D., & Alsdorf, D. (2007). The Shuttle Radar Topography Mission. *Reviews of Geophysics*,*45*(2).https://doi.org/https://doi.org/10.1029/2005RG000183

[18] Tadono, T., Takaku, J., Tsutsui, K., Oda, F., & Nagai, H. (2015, 26-31 July 2015). Status of "ALOS World 3D (AW3D)" global DSM generation. 2015 IEEE International Geoscience and Remote Sensing Symposium (IGARSS),

[19] Yamazaki, D., Ikeshima, D., Sosa, J., Bates, P. D., Allen, G. H., & Pavelsky, T. M. (2019). MERIT Hydro: A High-Resolution Global Hydrography Map Based on Latest Topography Dataset. *Water Resources Research*, *55*(6),5053-5073. https://doi.org/https://doi.org/10.1029/2019WR024873

[20] Anukularmphai, A., & Rivas, A. (2005). *A Case Study for Interlinked Coastal and River Basin Managementthe BangPakongRiverBasin*. https://doi.org/10.13140/RG.2.2.29230.92487

[21] Sangmanee, C., Wattayakorn, G., & Sojisuporn, P. (2013). Simulating changes in discharge and suspended sediment loads of the Bangpakong River, Thailand, driven by future climate change. *Maejo international journal of science and technology*, *2013*, 72-84.

[22] Prasertsri, W., Lu, J., Chen, X., Charoenjit, K., & Kaewwaen, W. (2020). *Simulation of Daily and Monthly Streamflow in Bang Pakong river basin Using the SWAT model*.

[23] Molle, F., Srijantr, T., & Promchote, P. (2009). *The Bang Pakong River Basin Committee : analysis and summaryofexperience*. https://doi.org/https://www.researchgate.net/publication/280637088_The_Bang_Pakong_River_Basin_Committee_analysis_and_summary_of_experience

24] Sayama, T., Ozawa, G., Kawakami, T., Nabesaka, S., & Fukami, K. (2012). Rainfall–runoff–inundation analysis of the 2010 Pakistan flood in the Kabul River basin. *Hydrological Sciences Journal-journal Des Sciences Hydrologiques - HYDROLOG SCI J*, *57*, 298-312. https://doi.org/10.1080/02626667.2011.644245

[25] James, W., Warinner, J., & Reedy, M. (2007). Application of the Green-Ampt Infiltration Equation to Watershed Modeling. *JAWRA Journal of the American Water Resources Association*, *28*, 623-635. https://doi.org/10.1111/j.1752-1688.1992.tb03182.x